Grasping Flat Objects by Exploiting Non-Convexity of the Object and Support Surface*

Iason Sarantopoulos[1,2], Yannis Koveos[2] and Zoe Doulgeri[1,2]

***Abstract*— In this paper we propose a grasp strategy which exploits environmental contact for grasping domestic flat objects placed or hinged on support surfaces. The proposed grasp strategy considers the non-convex geometry of the object-surface combination, as this appears in objects like plates on tables or handles on cupboards. Following the fact that state-of-the-art grasp planners fail to produce candidate grasps for flat objects due to the environmental constraint of the support surface, this work utilizes compliant interaction of the hand with the support surface, inspired by human grasp strategies.**

I. Introduction

The future service robot's aim is to operate in domestic environments and deal with everyday objects. This means that the robot should be able to grasp, manipulate, place and/or handover domestic objects. Many approaches have been proposed in the last decades towards this goal. In the recent review on grasp synthesis algorithms by Sahbani *et al.* [1], the authors classify the methodologies into *analytic* and *empirical* (or *data-driven*) with the latter further divided on whether they utilize object features or observation of humans during grasping. On the other hand, Bohg *et al* [2] group methodologies based on their assumptions on the target object, yielding three categories: *known objects*, *familiar objects* and *unknown objects*. For known objects, the robot has access to an *experience database* containing exact object models and their associated grasps, while familiar objects are assumed to be grasped in a similar to known objects manner.

All the above approaches assume a collision free space around the target object. However, in an average domestic environment, the objects are placed on support surfaces, which can be approximated by planes: tables, shelves, the kitchen counter, the floor etc. Any support surface pose an environmental constraint for current state-of-the-art grasp planners, like GraspIt! [3] or Simox [4], which attempt to synthesize grasps by avoiding collision with any other objects or the environment. The flatter an object is, the more difficult to grasp it without colliding with the support surface. As a result grasp planners may not produce a solution in the case of a small or flat object lying on a table [5]. Other works have shown promising results for grasping unknown objects in a cluttered environment, by using machine learning [6], [7]. Although the aforementioned works do not require the object model, as grasp planners do, they were only evaluated in non-flat objects, that do not need to explicity consider environmental constraints. On the other hand, the remarkable dexterity with which humans manipulate a variety of flat objects, stems from strategies that involve contact with the environment. Recent findings suggest that the utilization of environmental contact compensate for object pose estimation errors. Heinemann *et al.* [8] investigated the human grasping behavior, with respect to their use of contact constraints and discovered that humans compensated for the uncertainties introduced by impaired vision by using contact with the support surface. Therefore, the need to develop grasp strategies that incorporate contact with the support surfaces is imperative, particularly in the case of flat objects.

Research on robotic grasping has only recently focused on exploiting environmental constraints during grasp synthesis [5], [8]–[13]. In [11] the authors introduce the concept of *external dexterity*, which denotes the ability for in-hand manipulation using a very simple gripper, by utilizing the motions of the arm, object inertia and external contacts with the environment while [13] based on this work present an adaptive controller for pivoting an object. Elliot *et al.* [12] present a learning approach for reconfiguring objects in confined environments (shelves, drawers etc.) in order to make the objects graspable, by utilizing non-prehensile manipulation of the objects. Salvietti *et al.* [10] describe a mathematical framework for modeling the interaction between a compliant hand and its environment. Suitable soft hand designs has been proposed towards grasping with compliant environmental contact, like RBO hand [9] or Pisa IIT Softhand [14], [15]. Although compliant environmental contact is a necessary condition for grasping, is not sufficient as it is a prerequisite rather than a grasping strategy. Eppner *et al.* [9] were among the first who proposed constraint exploiting grasp strategies in order to achieve effective grasping namely the *surface-constrained* and the *edge* grasp strategy. The former focus on establishing an opposable grasp despite contacting the environment and hence it is confined to small objects for which the gripper's spread is adequate while the latter, utilizes non-prehensible manipulation prior to grasping.

In this work, we propose a contact exploiting grasp strategy for flat objects placed or screwed on a support surface which are characterized by non-convexity in their object-surface combination and thus may allow an opposable grasp. Typically, grasp planners fail to produce any feasible grasps for these cases, as the support surface is taken as an obstacle

*This work is funded by the EU Horizon 2020 research and innovation programme under grant agreement No 643433, project RAMCIP.

[1] Department of Electrical and Computer Engineering, Aristotle University of Thessaloniki, Thessaloniki, 54124 Greece iasons@auth.gr, doulgeri@eng.auth.gr

[2] Information Technologies Institute (ITI) Center of Research and Technology Hellas (CERTH) 57001 Thessaloniki, Greece {iasons, ykoveos, doulgeri}@iti.gr

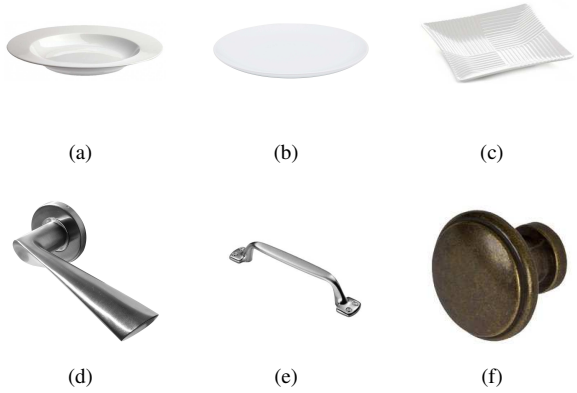

(a) (b) (c) (d) (e) (f)

Fig. 1. The relevant use cases. (a) A typical plate, (b) a plate without a rim, (c) a square plate, (d) a door handle, (e) a cupboard handle. (f) a knob

to be avoided. Examples of these objects that are typical of everyday domestic objects which a service robot will be required to grasp and manipulate are shown in Fig. 1.

In the remainder of this paper, we present the problem formulation (Section II), the proposed grasp strategy (Section III) and finally its experimental evaluation (Section IV). In Section V conclusions are drawn.

II. Problem Formulation

Our objective is to design a grasp strategy for objects with the following properties:

1) The object is placed or screwed on a planar support surface, a common case for domestic objects.
2) The object's height with respect to the support surface is relatively small intensifying the constraint of the support surface for grasping. Such an object is characterized as *flat*.
3) The combination of the object and the support surface presents a non-convex geometry.

In the context of this work, we assume the availability of a full point cloud for the object. For unknown objects the full point cloud can be obtained by 3D reconstruction of the scene by multiple views. In case only a partial view of the object is available, the object should be known so that a point cloud is extracted based on the known object after object detection and identification. In what follows, we present the way we model the robotic hand, the support surface, the target object and their combination.

A. The robotic hand

We consider a robotic hand with n fingers, a planar palm with its normal vector pointing inwards the workspace of the fingers and the frames $\{G\}$ and $\{N_j\}$ attached at the palm and fingertips, respectively. Frame $\{G\}$ is placed on the center of the palm with its z-axis aligned with palm's normal vector and the y-axis along the direction of an opposable finger synergy configuration. Frame $\{N_j\}$ is placed on the j-th fingertip, with y-axis along the distal link and the z-axis perpendicular to the distal link and on the plane defined by the distal link's rotational motion (Fig. 2a).

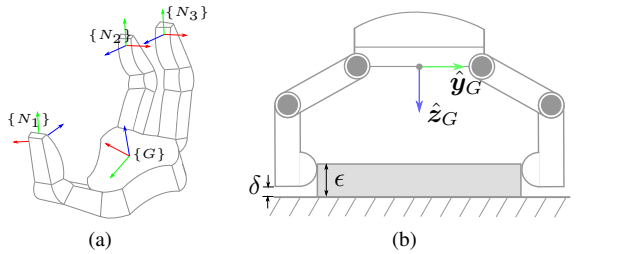

(a) (b)

Fig. 2. The robotic hand. (a) The frames considered on the hand by convention. With red, green, blue colors denoting x, y, z axes, respectively. (b) Visualization of the concept of flatness. The parameter ϵ is determined for each robotic hand.

B. The support surface

The support surface $\mathcal{S}$ is assumed to be rigid and is defined by its normal vector estimate, $\hat{\boldsymbol{s}}_n \in \mathbb{R}^3$, and a point $\boldsymbol{s}_p \in \mathbb{R}^3$ which belongs on the plane, usually provided by the perception system by a plethora of techniques.

C. The target object

We consider flat supported objects modeled as a set $\mathcal{O}$ of N object surface points in space, $\boldsymbol{o}_{p,i} \in \mathbb{R}^3, i = 1, ..., N$ typically provided by the perception system as a point cloud that are such that their maximum distance from the support surface is smaller than a threshold ϵ:

$$\max_{\boldsymbol{o}_{p,i} \in \mathcal{O}} \{\hat{\boldsymbol{s}}_n \cdot \boldsymbol{o}_{p,i} - |\hat{\boldsymbol{s}}_n \cdot \boldsymbol{s}_p|\} < \epsilon \tag{1}$$

The parameter ϵ denotes the minimum height of an object that can be grasped with the hand having an arbitrary small distance δ from the support plane (Fig. 2b). One practical way to determine ϵ is through sampling-based simulations for the given hand model and a scene of a rectangular primitive object placed on a plane, testing a number of hand configurations with opposable contact points on the object, for different heights of the rectangular object. Notice that, besides hand kinematics, ϵ depends also on the size and geometry of the fingertips; smaller fingertips allows grasps closer to the support surface.

D. Object-surface combination

Our approach extracts valuable information from the object-surface combination, determining the usability of the proposed grasp strategy on establishing an opposable grasp and the feasible approaching directions for this purpose. An opposable grasp is a typical pinch grasp, which allows the application of forces along the interaction line. Initially, the object points are projected on the support plane. Then, the *non-convex points*, which are the points lying in the empty space between the object and its projection on the support surface, are found (Fig. 3). These points are used during grasp execution, by placing at least one of the fingers within the space they define, in order to form an opposable finger synergy. As a final step, the reachability of the non-convex space by the fingers is evaluated. An example of this case is shown in Fig. 3d, which depicts a reversed plate. The non-convex points found within the cavity of the plate are not reachable due to the constraint of the object's surface.

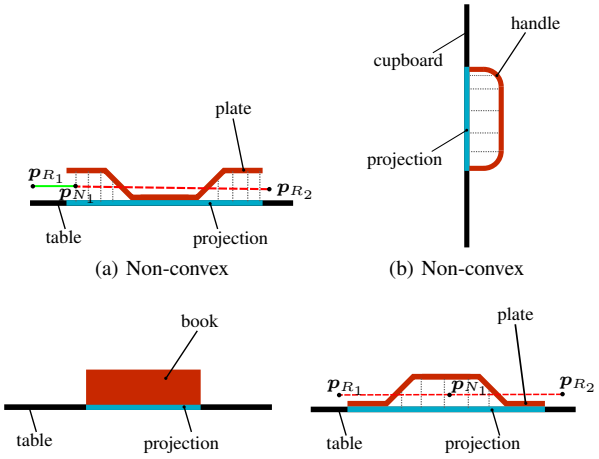

(a) Non-convex (b) Non-convex

(c) Convex (d) Convex

Fig. 3. Visualization of the non-convexity concept for different objects and surfaces. Each object is marked with red color and the orthogonal projection of the object on the surface with blue color. The figure depicts also the examples for the vectors $\boldsymbol{p}_N$, $\boldsymbol{p}_R$. (a) A plate placed on a table, (b) a handle on a cupboard, (c) a book on a table and (d) an inversed plate on a table.

In case we have feasible non-convex points we state that the object-surface combination is non-convex. The way to determine the reachable non-convex point is detailed in the following.

1) Object projection on surface: Define $\mathcal{S}_O$ as the set of points of the support surface produced by the orthogonal projection of $\boldsymbol{o}_{pi}$ on the surface:

$$\mathcal{S}_O = \{\boldsymbol{p} \in \mathbb{R}^3 \mid \boldsymbol{p} = \boldsymbol{g}(\boldsymbol{o}_{p,i}, \boldsymbol{s}_p, \hat{\boldsymbol{s}}_n)\} \tag{2}$$

where $\boldsymbol{g}$ gives the projected point on the support plane:

$$\boldsymbol{g}(\boldsymbol{o}_{p,i}, \boldsymbol{s}_p, \hat{\boldsymbol{s}}_n) = (I_3 - \hat{\boldsymbol{s}}_n \hat{\boldsymbol{s}}_n^T)(\boldsymbol{o}_{p,i} - \boldsymbol{s}_p) + \boldsymbol{s}_p \tag{3}$$

with $I_3 \in \mathbb{R}^{3\times3}$ denoting the identity matrix.

2) Non-convex points: Define $\mathcal{A} = \mathcal{S}_O \cup \mathcal{O}$ and $[\boldsymbol{p}_1, \boldsymbol{p}_2]$ the set of points in the line segment between $\boldsymbol{p}_1$ and $\boldsymbol{p}_2$:

$$[\boldsymbol{p_1}, \boldsymbol{p_2}] = \{\boldsymbol{p} \in \mathbb{R}^3 \mid \boldsymbol{p} = (1-\lambda)\boldsymbol{p}_1 + \lambda \boldsymbol{p}_2, 0 \leq \lambda \leq 1\}$$

Let us further define $\mathcal{N}$ as the set of non-convex points $\boldsymbol{p}_N$ between an object and its projection on the support surface:

$$\mathcal{N} = \{\boldsymbol{p}_N \in [\boldsymbol{p_1}, \boldsymbol{p_2}] \mid \min_{\boldsymbol{a}_i \in \mathcal{A}} \{|\boldsymbol{p}_N - \boldsymbol{a}_i|\} > \mu_1, \\ \forall \boldsymbol{p_1} \in \mathcal{O}, \boldsymbol{p_2} = \boldsymbol{g}(\boldsymbol{p}_1, \boldsymbol{s}_p, \hat{\boldsymbol{s}}_n)\} \tag{4}$$

In our case, parameter μ_1 depends on the hand in use. In particular, bigger fingertips will require higher values of μ_1, i.e. will need more clearance in order to establish contact points on the object by utilizing the non-convexity property (Fig. 4).

3) Reachable non-convex points: Consider $\mathcal{R}(\boldsymbol{p}_N)$ as a set of points $\boldsymbol{p}_R$ far from the non-convex point $\boldsymbol{p}_N$ and outside the object, i.e. points $\boldsymbol{p}_R$ have a distance from $\boldsymbol{p}_N$ greater than the maximum distance of $\boldsymbol{p}_N$ from any object point $\boldsymbol{o}_{p,i}$:

$$|\boldsymbol{p}_N - \boldsymbol{p_R}| > \max_{\boldsymbol{o}_{p,i} \in \mathcal{O}} |\boldsymbol{p}_N - \boldsymbol{o}_{p,i}| \tag{5}$$

Typically $\mathcal{R}(\boldsymbol{p}_N)$ set can be obtained by sampling a circular curve with radius r selected appropriately in order to satisfy (5), centered at the non convex point $\boldsymbol{p}_N$ and parallel to the support surface:

$$\mathcal{R}(\boldsymbol{p}_N) = \{\boldsymbol{p}_R \in \mathbb{R}^3 \mid |\boldsymbol{p}_N - \boldsymbol{p}_R| = r, (\boldsymbol{p}_N - \boldsymbol{p}_R)\hat{\boldsymbol{n}}_s = 0\} \tag{6}$$

A non-convex point can be reached by the fingers if the line segment between this point and a $\boldsymbol{p}_R$ point is not intercepted by the object's surface or the support surface. Define $\mathcal{N}_f$ the set of the pairs $\boldsymbol{p}_N, \boldsymbol{p}_R$:

$$\mathcal{N}_f = \{(\boldsymbol{p}_N, \boldsymbol{p}_R) \mid \min_{\boldsymbol{a}_i \in \mathcal{A}} \{|\boldsymbol{p}_s - \boldsymbol{a}_i|\} > \mu_2, \\ \forall \boldsymbol{p}_s \in [\boldsymbol{p}_N \quad \boldsymbol{p}_R]\} \tag{7}$$

where μ_2 a parameter, similar to μ_1, which assures clearance of the linear path towards $\boldsymbol{p}_N$ from $\boldsymbol{p}_R$. The larger the μ_2 value, the more the approaching directions that avoid the non-convex space's limits, meaning that wider fingers will be guided towards the centre of the non-convex space (Fig. 4). Examples for the reachability of the non-convex points can be found in Fig. 3a; pair $(\boldsymbol{p}_{N_1}, \boldsymbol{p}_{R_1})$ is a clear path and belongs to $\mathcal{N}_f$, in contrast to $(\boldsymbol{p}_{N_1}, \boldsymbol{p}_{R_2})$. Notice that in the case of the convex inversed plate of Fig. 3d no such pair exists and thus $\mathcal{N}_f = \emptyset$.

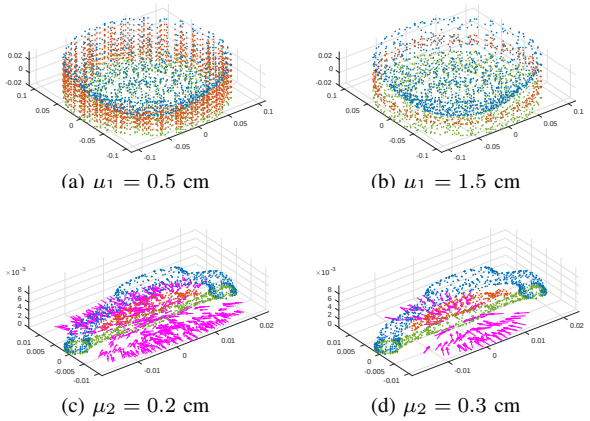

(a) $\mu_1 = 0.5$ cm (b) $\mu_1 = 1.5$ cm

(c) $\mu_2 = 0.2$ cm (d) $\mu_2 = 0.3$ cm

Fig. 4. The produced N and N_f sets for different values of the parameters μ_1, μ_2, for a plate and a handle, respectively. Blue color indicates the object's point cloud, green color the object's projection on the support surface, red color the non-convex points and purple colors the approaching directions of N_f.

III. The Proposed Grasp Strategy

The proposed grasp strategy is inspired by the way humans grasp objects in similar situations. It assumes that the hand in use is compliant and is attached to a compliant arm. The compliance on both the hand and the arm can be realized either actively, by a compliance controller or passively due to the intrinsic hardware characteristics. It further assumes that the fingertip pose is measurable by, e.g., proprioceptive sensors.

The strategies consist of three phases involving *Grasp State* targets defined as $[x_G \quad \boldsymbol{q}]$, where $x_G \in SE(3)$ the pose of the palm's frame $\{G\}$ and $\boldsymbol{q} \in \mathbb{R}^k$ the joint positions of the fingers, where k the total DOFs of the hand. The

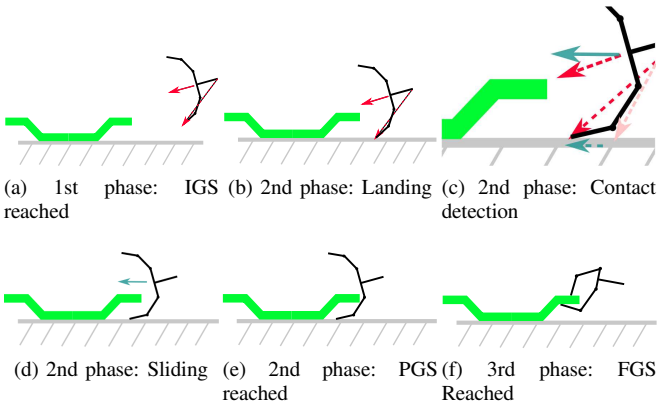

(a) 1st phase: IGS reached (b) 2nd phase: Landing (c) 2nd phase: Contact detection

(d) 2nd phase: Sliding (e) 2nd phase: PGS reached (f) 3rd phase: FGS Reached

Fig. 5. The concept of the proposed strategy. (a) The hand having reached the selected IGS it approaches the support surface with a predefined trajectory, (b) The hand establishes contact with the support surface, (c) Since the fingers are compliant, the contact force with the support surface causes their displacement, (d) Due to the change of the fingers position the contact is recognized and a new direction is given to the arm. (e) The hand recognizes the contact with the object meaning that we have reached the PGS. (f) The object is grasped.

Initial Grasp State (IGS) is an arm hand configuration that does not involve external contacts in general, the *Pregrasp State (PGS)* involves finger contact with the environment and/or the object while in the *Final Grasp State (FGS)* the object is securely grasped and no longer supported by the surface. Grasp state target IGS is planned online, given the current scene, while PGS and FGS are dynamically achieved during execution by the action of the grasp controller. The achievement of the PGS and FGS in each strategy depends on the current measurable state of the arm/hand system.

As potential goals of the first phase, multiple IGSs are planned instead of one desired IGS to provide different grasp possibilities to be considered for reaching given other constraints like obstacles surrounding the target object or kinematic constraints of the robot. The assumption is that a module exists which selects an appropriate IGS which is feasible with respect to the obstacles and the robot/hand kinematic. State of the art motion planners, like *MoveIt!* [16], may be utilized to this purpose.

Fig. 5 depicts the concept of the strategy. After the hand reaches the selected IGS, moves towards the surface and establishes contact with the support surface with the back of its fingers. The contact with the support surface is detected by the displacement of the fingertips due to their compliance. Then it slides towards the object by maintaining contact with the surface, until the hand touches the object or the target non-convex point is reached. Finally the fingers are closing grasping the object. A more detailed description follows.

A. Reaching Initial Grasp State

For this strategy, given a predefined finger configuration, we produce a set of IGSs which are computed from each pair $(\boldsymbol{p}_N, \boldsymbol{p}_R) \in \mathcal{N}_f$, that are defined in (4), (5), (6), (7), and easily calculated given the point cloud of the object $\mathcal{O}$ as described in the previous section for a desired hand approaching angle θ and a desired height h. Angle θ is the angle between the hand approaching direction and the linear path $(\boldsymbol{p}_N, \boldsymbol{p}_R) \in \mathcal{N}_f$, belonging on the same plane by design. Angle θ is dependent on the desired angle $\phi \in (0, \pi/2)$ of the distal link with the surface and the initial configuration of the finger that will initially come in contact with the support surface, in order to ensure finger displacement at contact and facilitate sliding. At the moment, it is determined offline in a way so that $\theta \in (0 \quad \pi)$ (Fig. 6b). The height h is the distance of $\{G\}$ from the support surface. The pose $x_G = [\boldsymbol{p}_G \quad R_G]$ of this state is calculated as follows:

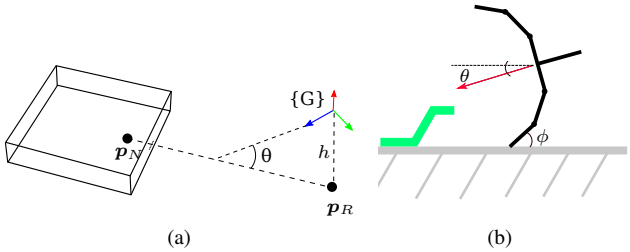

(a) (b)

Fig. 6. (a) One IGS for the proposed strategy where $(\boldsymbol{p}_N, \boldsymbol{p}_R) \in \mathcal{N}_f$ and h the desired height (b) The angles θ and ϕ

$$\boldsymbol{p}_G = \boldsymbol{p}_R + h\hat{\boldsymbol{n}}_s \tag{8}$$

$$R_G = \left[\hat{\boldsymbol{s}}_n \times \hat{\boldsymbol{k}} \quad \hat{\boldsymbol{s}}_n \quad \hat{\boldsymbol{k}}\right] Rot(x, \theta - \frac{\pi}{2}) \tag{9}$$

where $\hat{\boldsymbol{k}} = \frac{\boldsymbol{p}_N - \boldsymbol{p}_R}{|\boldsymbol{p}_N - \boldsymbol{p}_R|}$ is the unit direction along the linear path $(\boldsymbol{p}_N, \boldsymbol{p}_R) \in \mathcal{N}_f$ and $Rot(x, \theta - \frac{\pi}{2})$ is a rotation around the x-axis with angle $\theta - \frac{\pi}{2}$.

IGSs may be ranked based on the manipulability ellipsoid and its optimization along the direction of the subsequent motion (along the palm's normal) .

B. Reaching Pregrasp State

After the initial IGS has been reached the arm is commanded with velocity $\boldsymbol{v}_G$, updated at each control cycle by:

$$\boldsymbol{v}_G(k+1) = \begin{cases} \boldsymbol{v}_G(k), & \text{if } \Delta\boldsymbol{p}(k) = 0 \\ \Delta\boldsymbol{p}(k)|\boldsymbol{v}_G(k)|, & \text{if } \Delta\boldsymbol{p}(k) \neq 0 \end{cases} \tag{10}$$

where $\Delta\boldsymbol{p}(k)$, is the position displacement of the dominant fingertips w.r.t. the palm of the hand, with dominant fingers defined as those fingers that touch the support surface:

$$\Delta\boldsymbol{p}(k) = \frac{1}{|\mathcal{H}_f^r|} \sum_{j \in \mathcal{H}_f^r} (\boldsymbol{p}_{GN_j}(k) - \boldsymbol{p}_{GN_j}(k-1)) \tag{11}$$

where $\boldsymbol{p}_{GN_j}$ is the j-th fingertip frame position w.r.t. to the palm and $\mathcal{H}_f^r \subset \mathcal{H}_f$ the *dominant finger group* and $\mathcal{H}_f = \{1, 2, ..., n\}$ the set of the hand's fingers. In this work, the finger group is defined as two or more fingers that are controlled to act as one virtual finger with a tip defined at the mid-distance of the aligned finger tips that form the group. Initially, $\boldsymbol{v}_G(0)$ is set on the direction of the palm's normal which points towards the surface at a predefined magnitude. Notice that the contact is detected based on the motion of the

fingers w.r.t. the palm of the hand, due to their compliance. Detection is enabled by the continuous monitoring of the position displacement (Eq. (11)).

The PGS has been reached when at least one of the following stopping conditions holds:

- At least one of the dominant fingers senses force on the fingertips, i.e. $\sum_{j \in \mathcal{H}_f^r} F_{N_j}(t) \neq 0$.
- The force measurements on the arm's wrist, if available, exceeds a threshold in the direction of the non-convex approaching target.
- The hand's dominant fingertip has reached within a predefined vicinity around the target non-convex point.

C. Reaching Final Grasp State

After the PGS has been reached, the fingers start closing using the joint position controller of the fingers. Having obtained empirically a final configuration of the fingers, via kinesthetic demonstration, we provide joint trajectories on the fingers in order to reach this final configuration. Alternatively, a coordinated arm/hand velocity controller can be used. A failure during grasping is detected by the zero external forces on the fingertips. In case of failure, a higher level decision maker will be informed, in order to decide on the appropriate action, as to initiate again the grasping process.

IV. Experiments

Two different plates placed on a table and one cupboard handle are tested using two different setups: the 3-fingered BarrettHand BH8-282 equipped with torque sensors at its distal joints and the 4-finger Shadow Hand Lite [17] equipped with Optoforce force sensors [18] on its fingertips. Fig. 7 demonstrates the resulting approaching directions $(\boldsymbol{p}_R, \boldsymbol{p}_N) \in \mathcal{N}_f$ given the point clouds of a plate and a handle. Given the point cloud of each object and the support surface the algorithm produces the object-surface combination, finds the non-convex points and finally produces the approaching directions for the feasible non-convex points. Notice that in the case of the reversed plate, the object-surface combination is convex and no approaching directions are produced for this strategy. Given these approaching directions the IGSs of the strategy are produced as described in Section III-A. Fig. 8 demonstrates the reaching of PGS and FGS, as described in Sections III-B, III-C using Shadow Hand Lite. The video of all experiments can be found in the following link `https://youtu.be/poQytQ0PRd4`. During the approaching of the handle on an open cupboard the fingers succeed in maintaining contact with the support surface although the hinged door is moving under the exerted contact forces. This can be noticed in Fig. 8l-8q indicating the strategy's robustness to moving support surfaces.

The code for producing the approaching directions is available at `https://goo.gl/PSb9zD`.

V. Conclusions

In this work, we propose an approach for planning and executing grasps for flat objects exploiting contact with the support surface for cases the object-surface combination presents a non-convex geometry. The approach assumes a full point cloud availability and a compliant arm/hand and is robust to object and surface pose estimation errors. The proposed strategy is implemented and demonstrated experimentally with a KUKA LWR4+ arm equipped with Shadow Hand Lite for a plate on a table and a handle on a cupboard and is shown to be effective, even in cases of moving support surfaces.

References

[1] A. Sahbani, S. El-Khoury, and P. Bidaud, "An overview of 3D object grasp synthesis algorithms," *Robotics and Autonomous Systems*, vol. 60, no. 3, pp. 326–336, 2012.

[2] J. Bohg, A. Morales, T. Asfour, and D. Kragic, "Data-Driven Grasp Synthesis—A Survey," *IEEE Transactions on Robotics*, vol. 30, no. 2, pp. 289–309, 2013.

[3] B. Y. A. T. Miller, P. K. Allen, A. T. Miller, and P. K. Allen, "Graspit! a versatile simulator for robotic grasping," *IEEE Robotics & Automation Magazine*, vol. 11, no. 4, pp. 110–122, 2004.

[4] N. Vahrenkamp, M. Kröhnert, S. Ulbrich, T. Asfour, G. Metta, R. Dillmann, and G. Sandini, "Simox: A robotics toolbox for simulation, motion and grasp planning," in *Intelligent Autonomous Systems 12*. Springer, 2013, pp. 585–594.

[5] M. Kazemi, J.-S. Valois, J. A. Bagnell, and N. Pollard, "Robust Object Grasping Using Force Compliant Motion Primitives," *Proceedings of Robotics: Science and Systems*, pp. 1–8, 2012.

[6] A. Saxena, J. Driemeyer, and A. Ng, "Robotic grasping of novel objects using vision," *The International Journal of Robotics Research (IJRR)*, vol. 27, no. 2, pp. 157–173, 2008.

[7] A. ten Pas and R. Platt, "Using geometry to detect grasp poses in 3d point clouds," in *Int'l Symp. on Robotics Research*, 2015.

[8] F. Heinemann, S. Puhlmann, C. Eppner, M. Maertens, and O. Brock, "A Taxonomy of Human Grasping Behavior Suitable for Transfer to Robotic Hands," *IEEE International Conference on Robotics and Automation*, pp. 4286–4291, 2015.

[9] C. Eppner, R. Deimel, J. Álvarez-Ruiz, M. Maertens, and O. Brock, "Exploitation of environmental constraints in human and robotic grasping," *The International Journal of Robotics Research*, vol. 34, no. 7, pp. 1021–1038, 2015.

[10] G. Salvietti, M. Malvezzi, G. Gioioso, and D. Prattichizzo, "Modeling compliant grasps exploiting environmental constraints," *Proceedings - IEEE International Conference on Robotics and Automation*, vol. 2015-June, no. June, pp. 4941–4946, 2015.

[11] N. C. Dafle, A. Rodriguez, R. Paolini, B. Tang, S. S. Srinivasa, M. Erdmann, M. T. Mason, I. Lundberg, H. Staab, and T. Fuhlbrigge, "Extrinsic dexterity: In-hand manipulation with external forces," *Proceedings - IEEE International Conference on Robotics and Automation*, pp. 1578–1585, 2014.

[12] S. Elliott, M. Valente, and M. Cakmak, "Making objects graspable in confined environments through push and pull manipulation with a tool," *Proceedings - IEEE International Conference on Robotics and Automation*, vol. 2016-June, pp. 4851–4858, 2016.

[13] F. E. Vina, Y. Karayiannidis, C. Smith, and D. Kragic, "Adaptive Control for Pivoting with Visual and Tactile Feedback," *IEEE International Conference on Robotics and Automation*, 2016.

[14] M. G. Catalano, G. Grioli, E. Farnioli, A. Serio, C. Piazza, and A. Bicchi, "Adaptive Synergies for the Design and Control of the Pisa / IIT SoftHand," *International Journal of Robotics Research*, vol. 33, no. 5, pp. 768–782, 2014.

[15] M. Bonilla, E. Farnioli, C. Piazza, M. Catalano, G. Grioli, M. Garabini, M. Gabiccini, and A. Bicchi, "Grasping with Soft Hands," *IEEE-RAS International Conference on Humanoid Robots*, vol. 2015-Febru, pp. 581–587, 2015.

[16] I. A. Sucan and S. Chitta, "MoveIt!" [Online]. Available: http://moveit.ros.org

[17] "Shadow Hand Lite." [Online]. Available: https://www.shadowrobot.com/hand-lite/

[18] "Optoforce Sensor." [Online]. Available: http://optoforce.com/3dsensor/

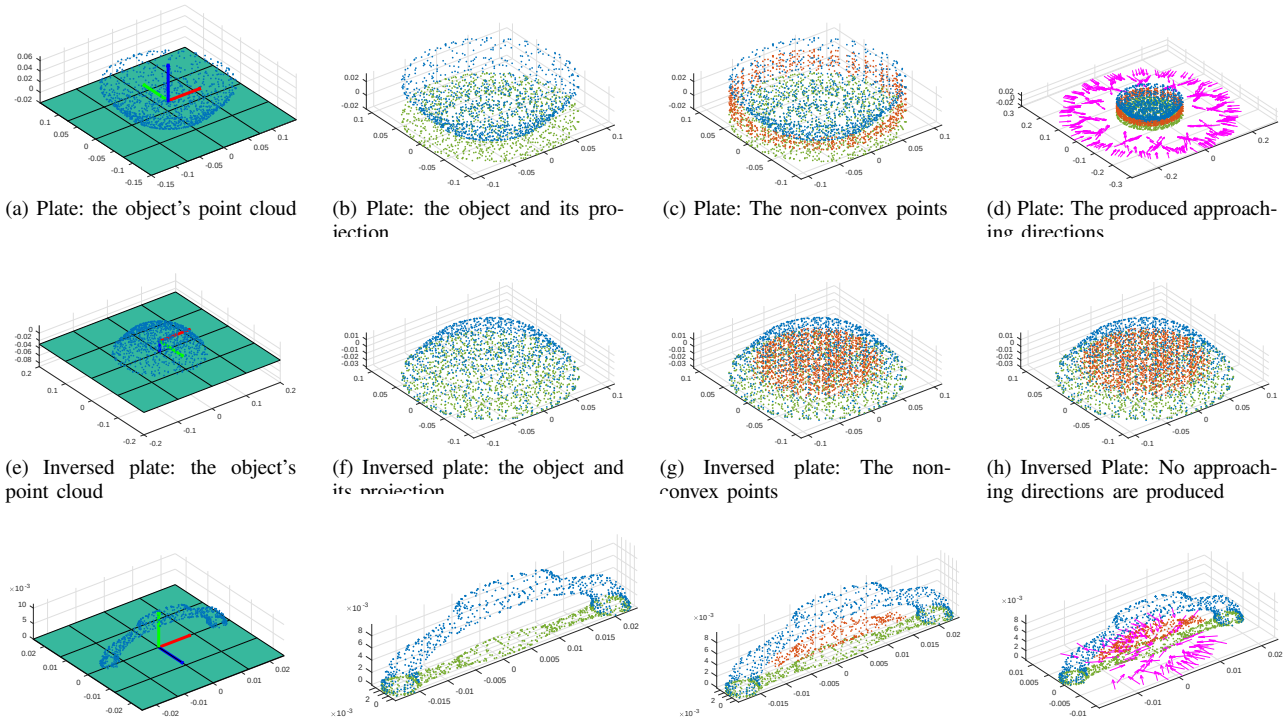

(a) Plate: the object's point cloud (b) Plate: the object and its projection (c) Plate: The non-convex points (d) Plate: The produced approaching directions

(e) Inversed plate: the object's point cloud (f) Inversed plate: the object and its projection (g) Inversed plate: The non-convex points (h) Inversed Plate: No approaching directions are produced

(i) Handle: the object's point cloud (j) Handle: the object and its projection (k) Handle: The non-convex points (l) Handle: The produced approaching directions

Fig. 7. The different phases for producing approaching directions from the object-surface combination for different cases. Each row demonstrates a different case: a plate placed on a table (a-d), a plate placed upside down on a table (e-h), a handle placed on a cupboard (i-l). Each column demonstrates a different phase: the object (point cloud) and the support surface (a,e,i), the object and its projection on the surface (b,f,j), the non-convex points (c,g,k) and finally the approaching directions for the feasible non-convex points (d,h,l). Blue color indicates the object's point cloud, green color the object's projection on the support surface, red color the non-convex points and purple the produced approaching directions.

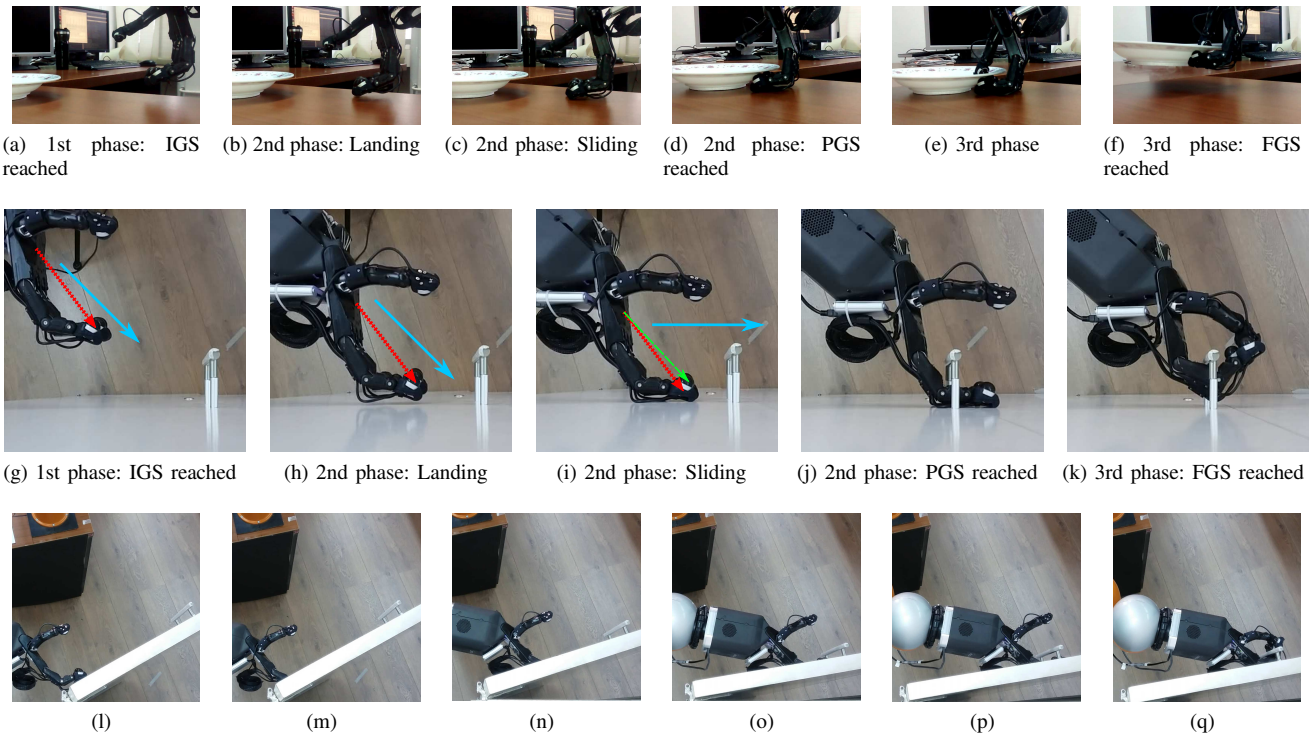

(a) 1st phase: IGS reached (b) 2nd phase: Landing (c) 2nd phase: Sliding (d) 2nd phase: PGS reached (e) 3rd phase (f) 3rd phase: FGS reached

(g) 1st phase: IGS reached (h) 2nd phase: Landing (i) 2nd phase: Sliding (j) 2nd phase: PGS reached (k) 3rd phase: FGS reached

(l) (m) (n) (o) (p) (q)

Fig. 8. Grasping a plate on a table and a handle on a cupboard using Shadow Hand Lite. (a)-(f) Grasping the plate using the proposed strategy. (g)-(k) Grasping a handle on a closet. The view of the experiment is from above the closet. The dotted red arrow denotes the initial position of the fingertip w.r.t the palm, while the dashed green arrow denotes the final position after contact with the surface. The blue solid arrow denotes the velocity of the hand. (l)-(q) Grasping the handle of an open cupboard.